

The MU2E experiment at Fermilab

C. Bloise, S. Bini, S. Ceravolo (Tech.), M. Cordelli (Ass.Senior), G. Corradi (Tech.)
E. Diociaiuti (Dott.), R. Donghia (AR), F. Fontana (Asso.), S. Giovannella, D. Hampai,
F. Happacher (Resp.), M.Martini (Asso.), A. Mengucci (Tech), S. Miscetti (Resp.Naz.),
B. Ponzio (Tech), G. Pileggi (Tech), A. Saputi (Tech), I. Sarra (Asso.), M. Ventura (Tech).

1 Introduction

During 2019, Mu2e has achieved many important milestones. The construction of the magnetic system and detectors has started in 2018 and continued in 2019. Indeed the magnetic system guides the "critical path" of the experiment. There was a 6-month delay in the project timeline during 2019 and the completion of the installation of the magnets has been postponed to the beginning of 2022. The experiment also suffered a financial crisis at the beginning of 2019, due to an additional cost of 9 M\$ due to both the delays in the construction of the magnets (+6 M \$) at General Atomics (GA) and to an unexpected increase in the cost. (+3 M \$) of the Transport Solenoid (TS) cryostat. This financial risk induced the experiment to deal directly with the management of the residual contingency by identifying the minimization of this risk in a "staging" procedure (in beam intensity and running time) of the experiment. This choice reduced the costs of the neutron shields and the initial background on the detector and allowed to save about 3 M\$. Even in this "staging" context, we continue organizing the transition phase between the construction of the detectors and magnets and the start of the commissioning operations (with and without beam). The start of the physics run is planned for 2023, within this current schedule and assuming: i) an initial reduction of the beam by a factor of two; ii) a gradual increase in the beam intensity near the shutdown of the accelerator, which is already planned to work and prepare the neutrino beam for Dune (currently scheduled for 2025-2026).

2 Magnetic system

The construction of the Transport Solenoid (TS) magnetic coils has been assigned to ASG Superconducting (Genoa) and it is proceeding satisfactorily. As a first positive result, all 52 coils have been completed and 40% of these have been already integrated in their modular mechanical structure. At the moment, ASG has delivered to Fermilab the first 7 complete modules, that are necessary for the construction of the first half of the TS (TSu, Upstream section). The preparation of the corresponding 6 modules of the second half (Downstream section) is already at an advanced level, but only some modules have been delivered. Figure 1 shows TSu/d bore and thermal shield eady. The first 4 module of TSu are assembled and the TSu will soon be completed.

Indeed the procedure is well ongoing and it is expected to have all the TS modules delivered to Fermilab within summer 2020 for the cooling test and for their installation. The construction of the Detector (DS) and Production Solenoid (PS) at General Atomics (GA) in the USA suffers from a longer delay. Fortunately, the technical problems highlighted during 2018 are now solved. After a year of testing, the superconducting cable winding procedure has been successfully defined and tested for both the Solenoid Detector (DS) and the Production Solenoid (PS). The official construction of the two magnets began in April 2019 and at the moment, the critical path of the whole experiment is still dominated by the delivery of these two magnets. The CD-4 achievement date (i.e. magnets and detectors completed and installed in the building) is currently estimated for the beginning of 2022.

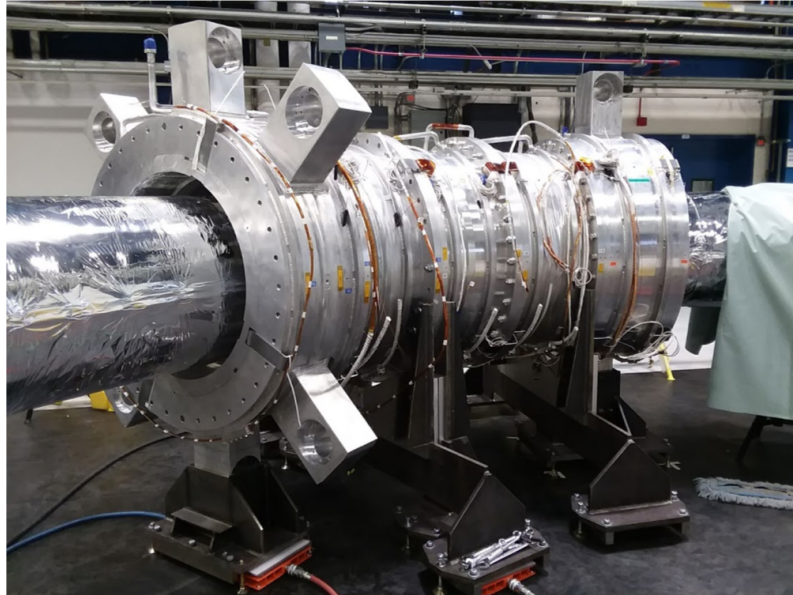


Figure 1: First four modules of the TSu installed and aligned. The first half of the TS will soon be complete.

3 Tracker and cosmic ray veto status

The Mu2e tracker system consists of approximately 20'000 panels of very thin straw tubes (5 mm in diameter, length varying within 40 and 100 cm, thickness of 15 μm) organized in 18 stations (2 floors per station, for 6 panels perfloor). The production of 216 panels has started in 2019, showing a certain number of difficulties. In particular, there are still problems in: i) "parallel" production, it is needed to obtain 4 functioning stations per time; ii) reduction of non-functioning channels per panel, which is still between 2-4%; iii) improve the gas leak rate and the level of HV discharges, that are not yet compatible with the vacuum operation requirement. The first 20 pre-production panels were produced by the end of 2019. Figure 2 shows the actual panel production workflow.

The construction begin is scheduled for the first months of 2020, but an overall delay of approximately 1 year for the completion of the detector is estimated (i.e. delivery to the experimental building within December 2021). In the meantime, both the assembly of the panels and the production of the electronic boards have started. Discussions on possible INFN contribute during the QC phase of the panels are ongoing, as well as for the implementation of plans. But the task assignment is still evolving. The veto detector for cosmic (CRV) consists of 330 m^2 extruded scintillators about 4 m long, in which two WLS fibers are inserted in order to collect the scintillation light on Hamamatsu SiPM ($2 \times 2 \text{ mm}^2$). The production is organized to construct the counters as first. Then they are grouped in modules containing 4 counters. The scintillators construction has been completed and the counters production is already in an advanced phase. The modules production completion is planned by mid 2021. The assembly will take place at the end of the magnets assembly phase and the construction is planned following the construction of the roof concrete walls.

Panel Production Stations

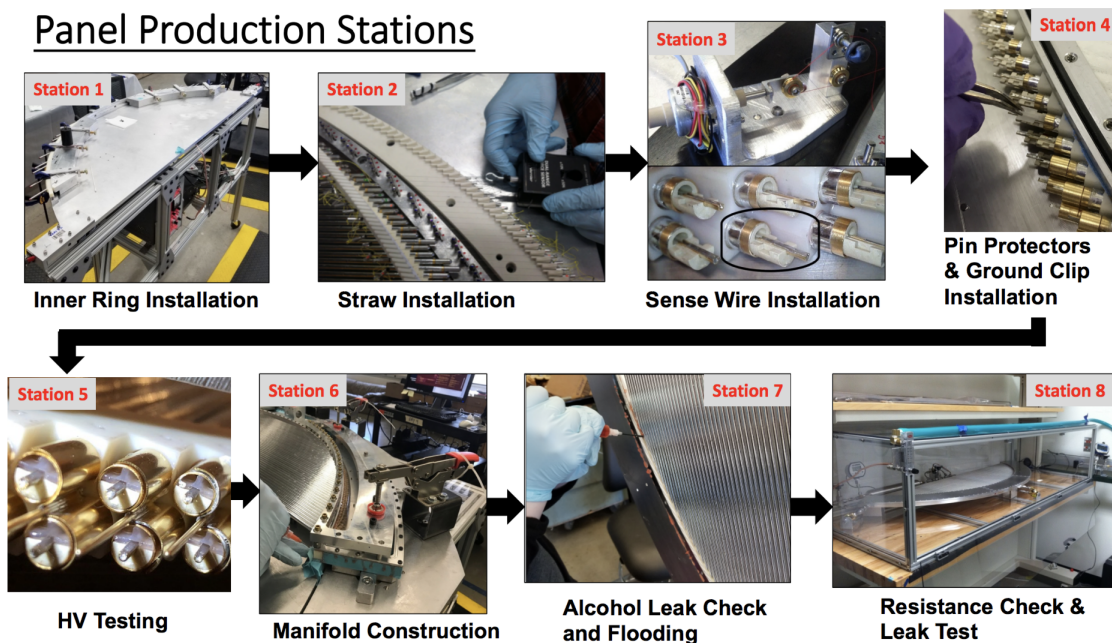


Figure 2: Workflow stations for a single tracker panel production.

4 Calorimeter state of art

The Mu2e calorimeter is composed by two annular disks containing 674 pure CsI crystals each. Each crystal is readout by 2 UV-extended Mu2e-SiPMs (a Mu2e SiPM is a custom array of 6 SiPMs cells of $6 \times 6 \text{ mm}^2$ dimensions). This detector design is the result of a long and intense R&D phase, that has been led by the LNF-INFN group. At the moment of writing, the production phase of all these components has started.

4.1 Crystal and SiPM production phase

The production of the calorimeter components has started in 2018 and continued during 2019, in order to test all the 1450 crystals and 4000 SiPMs needed for the two disks. Both productions were shipped directly from the manufacturers to Fermilab, where the Quality Assurance and Control survey were organized and managed by the INFN team. At the moment of writing, 85% of the total crystal production have been completely characterized, as reported in Figure 3

Once at Fermilab, crystals were first of all subject to an optical survey, in order to check polishing and scratches on the surfaces, and to a dimensional measurement using a Dimensional Control Machine, to check the congruence of the thickness, length and parallelepiped shape within a tolerance of $100 \mu\text{m}$. All the crystals mechanical measurements performed are reported and summarized in Figure 4.

The situation was very different between the two selected producers assigned with an international tender (Siccas from China and Saint Gobain from France). SICCAS produced all 725 crystals within May 2019, with one month only of delay (compared to the schedule). The crystals were perfect both from an optical and dimensional point of view, and complying to the calorimeter requirements. On the contrary, the crystals of St. Gobain showed evident problems in dimensional precision.

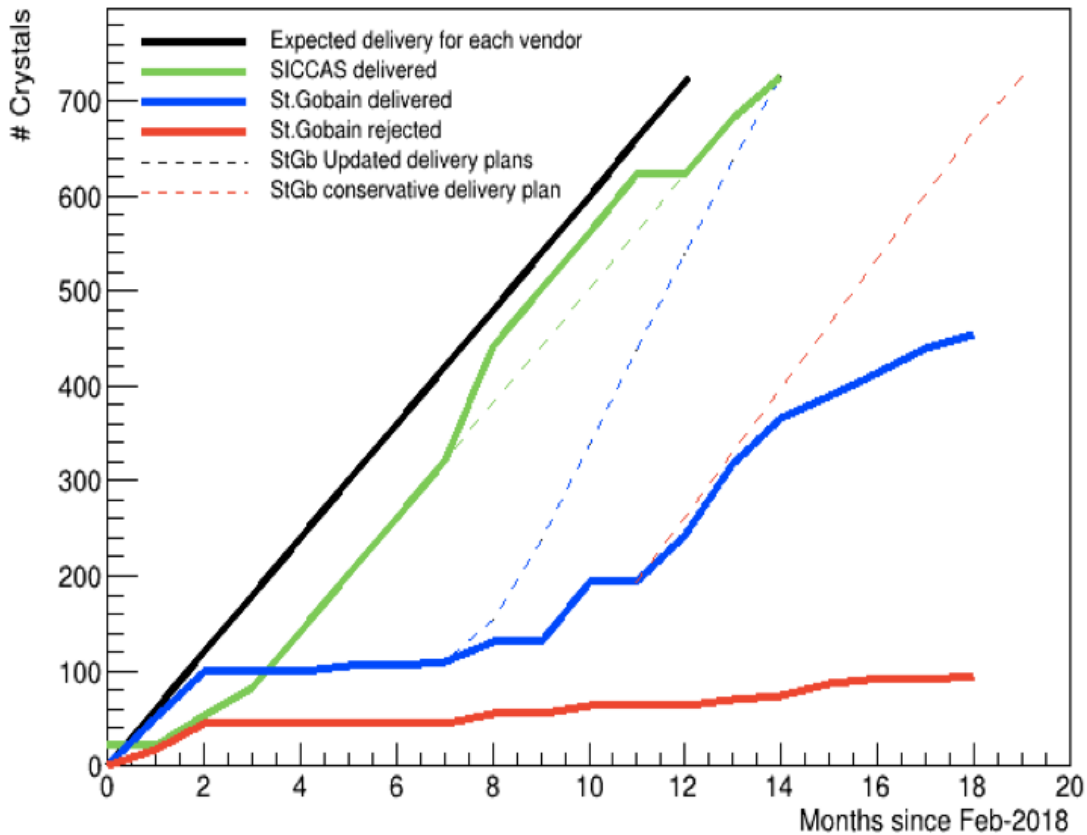


Figure 3: Crystal delivery plan.

After alternating successes and failures, just 400 crystals could be considered acceptable. So that, it was agreed to close the contract in August 2019 and the production of the last 325 pieces has been re-assigned to SICCAS, which will ship the new production to FNAL within spring 2020.

We summarize in the following the 5 automatized custom stations used for the QA tests for all the components:

- Crystals QA, a station for crystals optical test capable of determining light output in pe/MeV , uniformity of the longitudinal response and ratio between the fast and slow emission component (see Figure 5);
- Radiation Induced Noise, a dedicated station has been built to measure the fluorescence induced on the crystals when irradiated with a ^{60}Co source (see Figure 6);
- SiPM dimensional control, a station dedicated to the dimensional measurement of the thickness and pins positioning for the Mu2e-SiPM arrays;
- SiPM QA, a station for measuring parameters characterizing the SiPM in a vacuum chamber (i.e. curve IV, the operating voltage value V_{op} , and the product Gain x PDE) at three temperature values (-10, 0, 25 C);

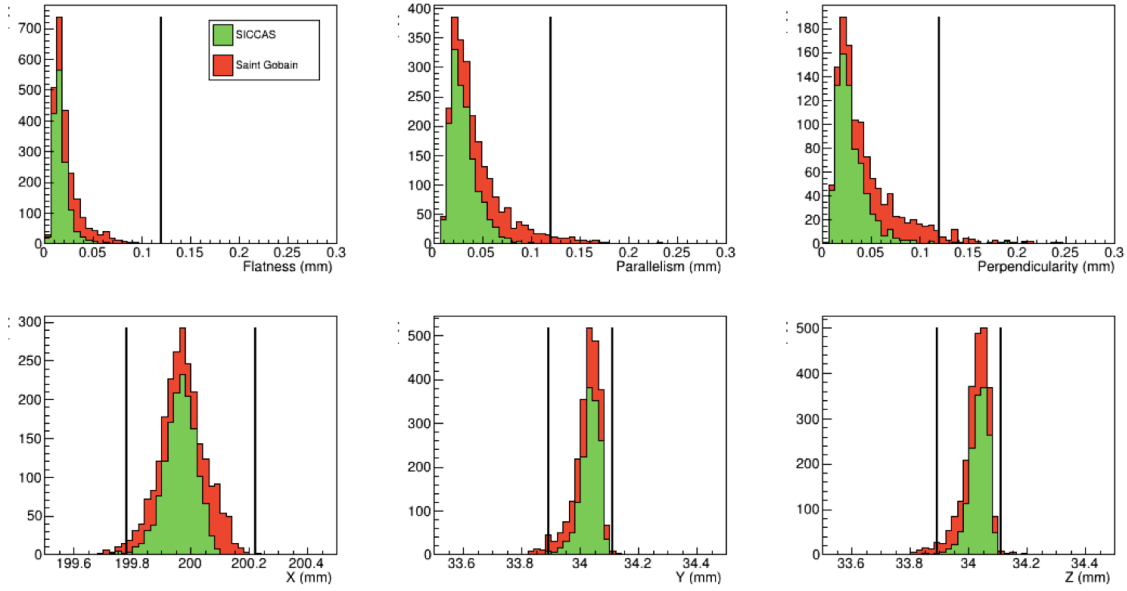


Figure 4: Crystals dimensiona measurements performed with a CMM machine.

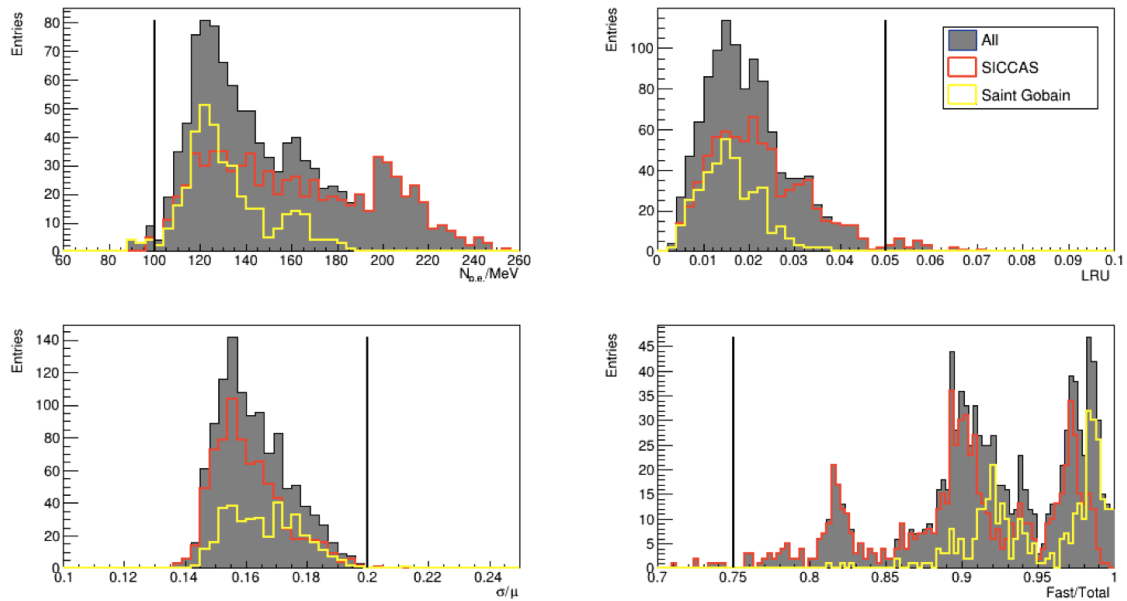


Figure 5: Crystals optical properties evaluated with 511 keV electrons from a ^{22}Na source scan on the longitudinal axis and a PMT readout.

- SiPM Mean Time to Failure, a station for the measurement of the MTTF of 15/batch randomly selected SiPM (operating for 3 weeks at a temperature of 65 C), in case of no-failure, this test corresponds to the achievement of a MTTF of one million hours.

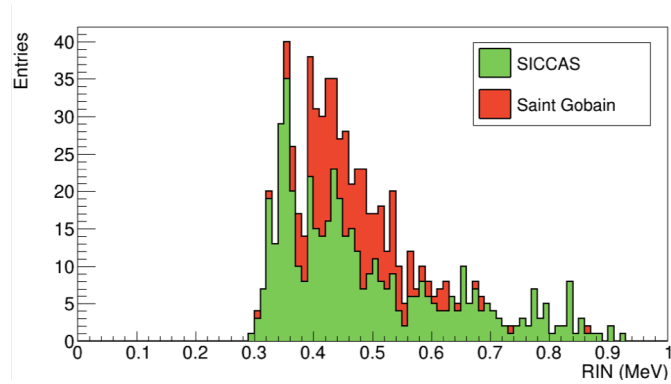


Figure 6: Crystals Radiation Induced Noise evaluated using a ^{60}Co source.

Concerning SiPMs, the production has been completed in May 2019 (for a total of 3950 Mu2e-SiPMs), with a rejected rate lower than 5 per mill. Indeed the operating parameters were in excellent agreement with those provided by Hamamatsu, for each of the 6 cells of the Mu2e-SiPMs produced, and largely within the experimental requirements. The QA results on breakdown voltages are reported in Figure 7.

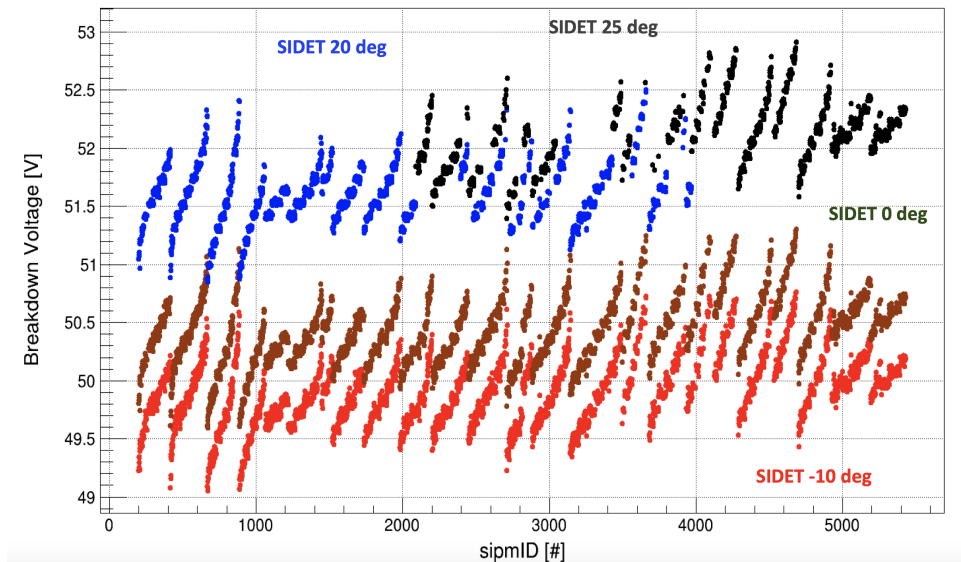


Figure 7: SiPM breakdown voltage measurements performed at SiDET at different temperature values.

Selection requirements have been applied on the RMS over the six cells in the Mu2e-SiPM array. Figure 8 shows the RMS over the breakdown voltage, dark current (at breakdown voltage) and on the Gain times PDE product. The red line represents the requirement limit, which are: i) RMS of V_{br} below the 0.5% limit; ii) RMS of $I_{dark}(V_{op}) < 15\%$ at 25 C; ii) Gain x PDE of each cell greater than 2×10^5 .

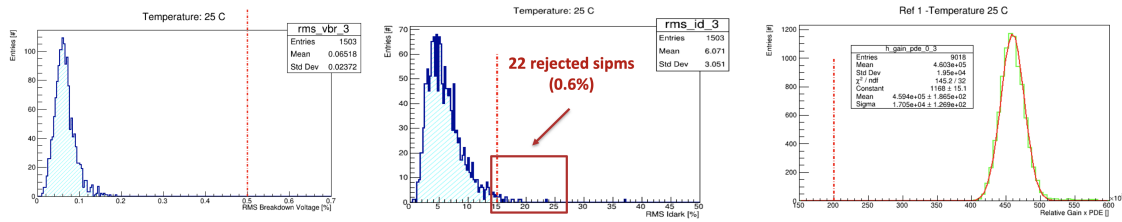


Figure 8: SiPM breakdown voltage measurements performed at SiDET at different temperature values.

The final MTTF value obtained is larger than 12 million hours (the experimental requirement is 1 million), as reported in Figure 9.

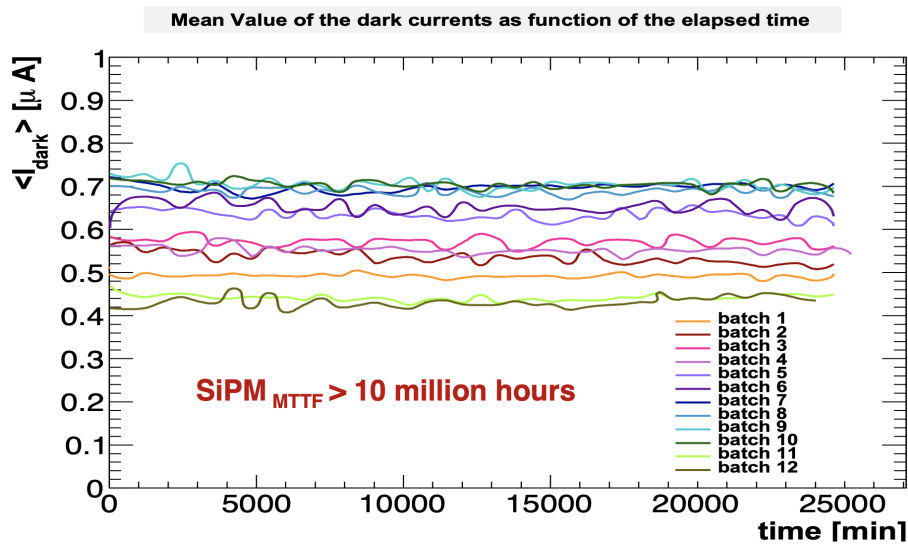


Figure 9: Dark current of each batch SiPMs as a function of the elapsed time. After 18 days operating at 65 C, no failure have been observed in all the Mu2e-SiPMs tested..

Neutron irradiation was carried out at HZDR laboratory in Dresden, randomly selecting 5 sensors per batch of 300 pieces. The SiPMs have been exposed up to a total fluence of 1.5×10^{12} n/cm² and the growth of the dark current values was consistent with the measurements made in the pre-production phase and with the electronic board requirement of 2 mA at 0 C. In September 2019, an additional irradiation test has been carried out at the FNG facility of ENEA (Frascati Neutron Generator) with 14 MeV neutron. This check revealed a scale problem of about a factor two between the fluence estimated at HZDR and those estimated at FNG. The SiPM+electronic cooling system, have been designed and pushed to operate down to -10 C, in order to reduce the dark current irradiation noise during the experiment data taking.

4.2 Electronic boards production phase (PCB and CRR)

In 2019 we completed the design and construction of the Front End Electronic and of the digitalization (DIRAC) systems. The FEE boards are directly connected to the Mu2e-SiPMs, as shown in Figure 10 (left). Instead, DIRAC boards are used to acquire signals and they are arranged in crates arranged over the calorimeter disks. The expected TID value for the digital part has

been reduced down to about 12 krad in the crates, thanks to an effective shielding of the crates consisting of WCu plates. While it has remained around 100 krad in the FEE area. A very intense irradiation campaign has been performed to accurately choose and insert in the final design rad-hard electronic components, resistant to both to ionizing dose (TID) and neutron and proton fluences. So that several tests have been performed, starting in 2018 and continuing for much of 2019 too, allowing more precise definition of an electronic design resistant to both ionizing dose (TID) and neutron and proton flux.



Figure 10: Left: CAD drawing of a FEE board connected to a Mu2e-SiPM. Right: Picture of Mezzanina and DIRAC boards connected together.

Concerning the FEE design, we tested particular digital elements, such as ADC and DAC, which are used for reading and regulating high voltage and for monitoring current and temperature. We decided to use ADC and DAC components from Texas Instrument, that significantly improved the FEE functionality, showing a variation of about 3% at the final TID. In July 2019, the PCB design review was carried out and it was concluded with satisfying results, with the only recommendation to check the possibility of using bias voltages up to 200 V in vacuum. A Paschen effect test has been performed at LNF, by varying the bias voltages from 0 to 800 V at several vacuum levels, between 10^{-2} and 10^{-4} Torr. The test has shown that the calorimeter electronics do not suffer from vacuum discharges and the breakdown voltage at the minimum point of the curve (10-20 Torr) is around 400 V. This value does not meet the requirements decided by the integration group considering a safety factor of 2. For this reason an Interlock system for HVs is being integrated that will be connected to the pressure value in the DS. In November 2019, the CRE(CRR?) for the FEE design was then carried out with positive results, allowing the completion of the production tender in mid-December 2019. The final production phase has started in the early months of 2020 after having completed a third irradiation test on pre-production boards.

Regarding the DIRAC digitization board, the first complete slice test of the calorimeter (crystal+SiPMs+FEEs+MB+DIRAC) was performed in the first half of 2019, by connecting a certain number of crystals, SiPMs and FEE-V3 boards with voltage regulation given by the Mezzanine board and digital reading via the DIRAC-V1 (Figure 10, right). This version of the digitizer is based and managed by a SmartFusion 2 FPGA (MicroSemi) and uses a traditional optical receiver. Figure 11 shows the comparison between data acquired with the DIRAC-V1 and those acquired with a commercial CAEN digitizer with the same sampling rate of 200 Msps (5 ns). It demonstrates a completely satisfying result.

During 2019 the design of the DIRAC-V2 was completed. The interface section with the Mezzanine and the ADC system for reading the signals remained unchanged, while many modifications were made regarding the DC-DC converter, the FPGA and the optical transceiver used. These 3 components have been replaced with improved rad-hard versions and for integration similarity with the tracking electronic system. For the DC-DC converter, irradiation tests and B-Field measurements have shown that the LMZ33606 selected model is resistant to high neutron fluxes,

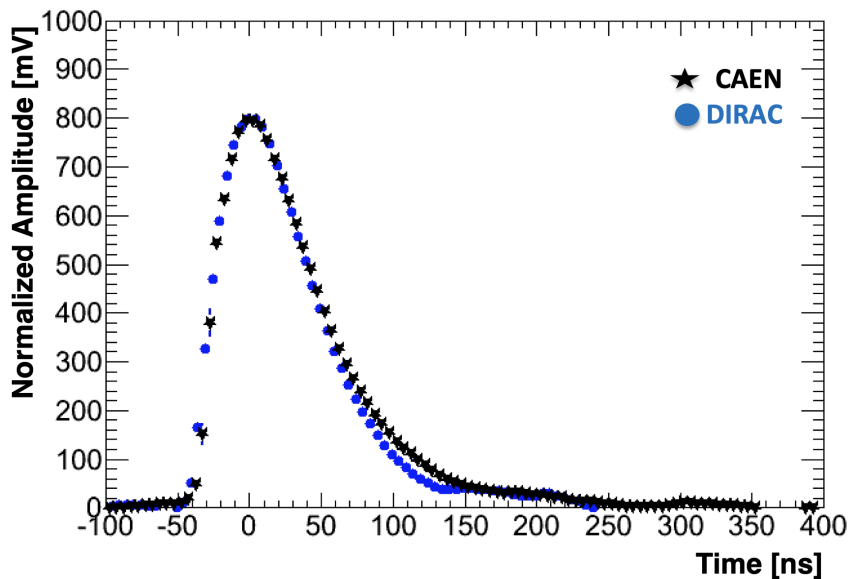


Figure 11: Slice test waveforms acquired with a DIRAC-v1 board (blue) and a commercial CAEN digitizer (black), in same running conditions.

for ionizing doses up to 50 krad and works perfectly in a field of 1 Tesla. For the FPGA, the MicroSemi Polar Fire was used in analogy with the choices made for the tracker system. Another common choice between tracker and calorimeter regards the optical link. Both the detectors will use the VTRX chip developed at CERN. The design of the DIRAC-V2 was completed in late summer. The construction of the first 5 prototypes has followed in November, as well as defining the specifications used for the production of the 160 cards for the calorimeter. The preliminary functionality tests of cards, began in December, showed that all cards comply the expectations. The next step planned for 2020 is to complete the firmware for data reading and for integration into the TDAQ.

4.3 Completion of mechanical structure drawings.

We had bi-weekly meetings at Fermilab during 2019 to address all the issues concerning the integration of the calorimeter mechanical layout in the Detector Solenoid environment. We analyzed in detail all the possible interferences among the calorimeter and the other components of the Muon Beam line, like the tracker, the tracker services, the cooling pipes and electrical cables, the Detector Solenoid and the rail system. The effort has implied the finalisation of the executable drawings of all the main components of the calorimeter. Before the start of the manufacturing of the mechanical parts, the Mu2e collaboration required us to undergo a careful scrutiny by an independent committee. Therefore, in May 2019 we had the Construction Readiness Review and all the details of the mechanics have been discussed and eventually agreed upon. The successful completion of the Review has represented the green light for the manufacturing of the calorimeter components.

All the materials used for the construction of each component had to comply with the out-gassing properties required by the experiment that has to work at 10^{-4} Torr vacuum; therefore we tested in Frascati the behaviour of all the proposed materials. Only the Aluminum foam pro-

posed for the construction of the Source plate has failed this test and we replaced it with an Al honeycomb designed for space applications.

As shown in Figure 12, each calorimeter annulus is composed of:

- an Outer monolithic stepped structural Al ring;
- an inner Carbon Fiber stepped ring;
- pair of feet with X-Y adjustment
- a Carbon Fiber front plate with an embedded pipes system for the flowing of a calibration radioactive fluorinert fluid;
- a PEEK back plate for the housing of the photosensors and their FEE electronics, with an embedded cooling circuit made of copper pipes;
- 10 digital electronic crates with a cooling serpentine connected to the main cooling pipes;
- 674 CsI crystals wrapped with Tyvek and black tedlar;
- 2 SiPM's and FEE electronics per crystal integrated in a copper holder and Faraday cage box (zoomed picture);
- a Laser calibration system.
- FEE cabling, HV/LV cabling and DAQ fibers

We have provided the manufacturing companies, that had the individual tenders assigned, with all the quoted drawings and kept interacting with them to assess and agree on the best construction techniques. At the end of 2019 all the parts of the calorimeter began to be produced.

We have designed the stand used to hold the calorimeter supports during the assembly of crystals, cooling and electronics. Two stands are being built and will also be used for transportation purposes during the move of the Calorimeter Annuli from the assembly room at Sidet (FNAL) to the Mu2e main hall. They will be provided with shock absorbers to reduce the vibrations along the 1 mile drive.

Furthermore, with the detailing of all the components, we have written a full installation procedure for the assembly and quality control of each individual annulus. To this end, the practice of the installation of the whole array of fake crystals in the real size mock-up in Frascati has been very instructive. We have assessed the technique and procedure for the gluing of the SiPM to the copper holder; this, being in thermal contact with the cooling lines of the FEE plate, takes care of the thermalization of the SiPM and power dissipation of FEE boards. We have built the tooling set to precisely glue the SiPM to the holders and tested the procedure with few holders prototypes and bad SiPM discarded by the SiPM QA procedure.

The Laser calibration system layout is final. We have built the distribution chain for the laser light that shines each of the 674 crystals via quartz fibers and diffusive integrating spheres. The reference pin-diodes and read out for normalization measurement has also been tested and all the hardware is being purchased.

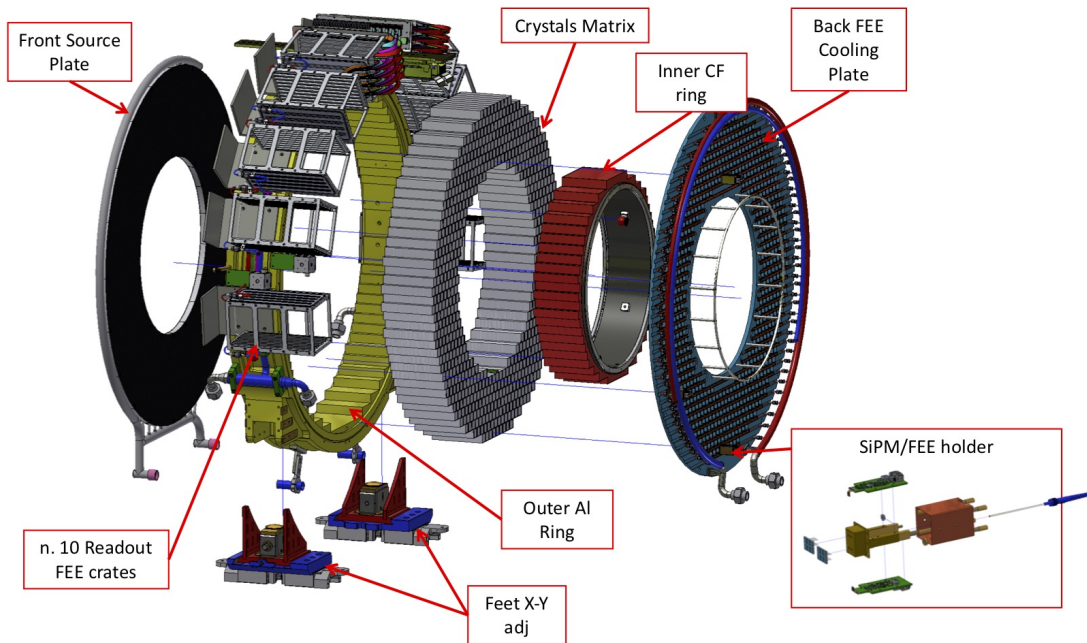


Figure 12: Exploded view of all the mechanical components.

5 Software and Data Analysis

In 2019 the INFN group has been also involved in several software tasks, concerning the reconstruction and analysis of simulated samples and the TDAQ. First of all, the simulation of the calorimeter response have been completed exploiting the Module-0 test with an electron beam, using the data-MC comparison used just for these electron samples. The same work has been performed on the reconstruction of the data taken with a laser trigger or with a cosmic ray trigger on the Module-0 in different conditions: in vacuum, with sensors irradiated or not and at different temperature values. These studies have shown that the technical calorimeter requirements will be satisfied also at the end of the physics run, just cooling the detector sensors down to temperatures of around -10°C .

For the Trigger DAQ system (TDAQ) there have been important developments concerning two main aspects:

- integration and development of the firmware for the DIRAC cards;
- integration of the Slow Control and Online Monitoring (DQM) processes in the run-control of the experiment (OTSDAQ).

Additional work is ongoing on the study of calibration strategies:

- simulation of the radioactive source used to equalize and calibrate the channel-to-channel response at 6 MeV;

- simulation of cosmic rays MIPs for calibrating the energy response of all the channels using the energy loss per unit distance and for determining the channels timing alignment using an iterative procedure for the minimization of time offsets (PhD thesis)
- simulation of electrons coming from muons decay in orbit (DIOs) for a calorimeter energy calibration, related to the tracker response.

Additional studies were carried out for the following physics channels as subjects of master or doctoral research thesis. In particular, a first estimate of the rate of Radiative Pion Capture (RPC) on the calorimeter as a function of the data acquisition window was performed. Moreover, knowing from the test beam the detector response of the calorimeter it was possible to start the study of the procedure for the fit to the RPC spectrum, as reported in Figure 13. A first estimate of the

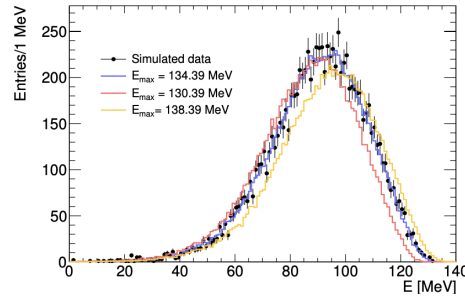


Figure 13: Expected RPC spectrum obtained with the calorimeter with different endpoint values.

prominent background to the $\mu^- \rightarrow e+$ conversion process led to the evaluation of a preliminary sensitivity at a level of $\sim 10^{-16}$, which could improve by 3-4 orders of magnitude the current best limit. In figure 14 (left) the distribution of the dominant backgrounds as well as the signal spectrum are reported.

As shown in Figure 14 (right) the sensitivity has a strong dependence on the endpoint of the Radiative Muon Capture (RMC) distribution. With the calorimeter it is possible to measure the EMC spectrum obtaining enough statistics in the signal region in only one month of data taking, allowing a better knowledge of the tails of this spectrum. Many of these studies will continue in 2020 too:

- study of the photon spectrum for Radiative Pionic Capture (Degree thesis);
- study of the photon spectrum for RMC;
- study of sensitivity for the conversion process cLFV $\mu^- \rightarrow e^-$ (degree thesis);
- study of the sensitivity for the cLFV and LNV in the $\mu^- \rightarrow e+$ conversion process (PhD thesis);
- feasibility study for the use of high quality sparkling crystals (LYSO, LABR) read with SiPM for the measurement of normalization photons linked to the muon capture process;
- study of proton reconstruction for the normalization measurement related to the muon capture process (Degree thesis).

6 List of Conference talks/prices by LNF authors in Year 2019

Talks:

1. S. Giovannella, "The Detectors of the Mu2e Experiment", IPRD 2019, Graduate College Santa Chiara, Siena, Italy.
2. I. Sarra, "The Mu2e e.m. calorimeter: crystals and SiPMs production status", SCINT 2019, Tohoku University, Katahira, Japan.
3. F. Happacher, "The Mu2e Crystal Calorimeter", SCTF 2019, Russian Academy of Sciences, Moscow, Russian Federation.
4. R.Donghia, "The Mu2e experiment", SIF National Congress 2019, GSSI, L'Aquila, Italy.
5. S. Miscetti, "Status of the Mu2e experiment", FCCP 2019, Villa Orlandi, Capri, Italy.
6. E. Diociaiuti, " $\mu^- \rightarrow e^-$ conversion and the Mu2e experiment at Fermilab", EPS 2019, International Convention Center and Ghent University, Ghent, Belgium.
7. E. Diociaiuti, "Production and quality assurance of Mu2e calorimeter CsI crystals" (poster), New Perspective 2019, Fermilab, Batavia, IL, USA.
8. R.Donghia, "Design and status of the Mu2e crystal calorimeter", New Perspective 2019, Fermilab, Batavia, IL, USA.
9. F. Happacher, "The Mu2e Experiment", WONP 2019, Hotel Plaza, La Habana, Cuba.
10. R. Donghia, "Design and status of the Mu2e crystal electromagnetic calorimeter", VCI 2019, Vienna University of Technology, Wien, Austria.

Publications:

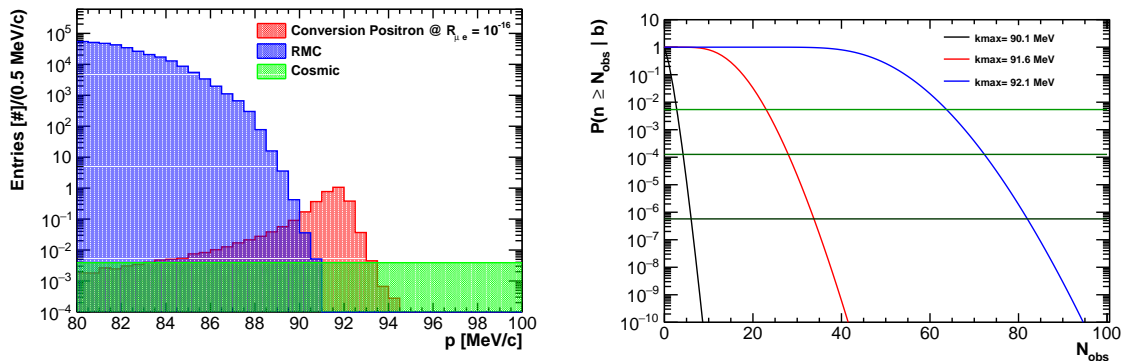


Figure 14: Left: Momentum distribution for background and Conversion Positron, assuming $R_{\mu e} = 10^{-16}$. Distributions are normalized to the Mu2e expected number of protons on target in 3 years of running, $N_{POT} = 3.6 \times 10^{20}$. Right: probability curves $\mathcal{P}(n \geq n_{obs} | b)$ used to evaluate the discovery sensitivity for three values of endpoint (90.1 MeV, 91.6 MeV and 92.1 MeV). N_{obs} corresponding to a $\mathcal{P}(n \geq n_{obs} | b) = 5.7 \times 10^{-7}$ (5σ) represents the number of event corresponding to a discovery.

1. N. Atanov et al., "Final design and current status of the Mu2e crystal calorimeter", 2018 IEEE NSS/MIC, DOI: 10.1109/NSSMIC.2018.8824316, published on 5 September 2019.
2. N. Atanov et al., "Design and status of the Mu2e crystal calorimeter", NIM A 958 1 April 2020, 162140, <https://doi.org/10.1016/j.nima.2019.04.094>.
3. N. Atanov et al., "The Mu2e calorimeter: Quality assurance of production crystals and SiPMs", NIM A 936 (2019) 154, : 31 January 2019
4. N. Atanov, "Mu2e Calorimeter Readout System", NIM A 936 (2019) 333, published on 31 January 2019
5. N. Atanov et al., "Design and test of the Mu2e undoped CsI + SiPM crystal calorimeter, NIM A 936 (2019) 94-97, DOI: 10.1016/j.nima.2018.09.043

Prices:

1. E. Diociaiuti, Della Riccia research grant for young Italian researcher.
2. R. Donghia, NIM A Young Scientist award for the best oral presentation at VCI2019.